

# Potentiometric, Electrochemical, and Fluorescence Study of the Coordination Properties of the Monomeric and Dimeric Complexes of Eu(III) with Nucleobases and PIPES

Hassan A. Azab,<sup>\*,†</sup> S. S. Al-Deyab,<sup>§</sup> Zeinab M. Anwar,<sup>†</sup> and Rasha M. Kamel<sup>†</sup>

<sup>†</sup>Chemistry Department, Faculty of Science, Suez Canal University, Ismailia 41522, Egypt

<sup>‡</sup>Chemistry Department, Faculty of Science, Suez Canal University, Suez, Egypt

<sup>§</sup>Department of Chemistry, Petrochemical Research Chair, King Saud University, P.O. Box 2455, Riyadh 11451, Saudi Arabia

**ABSTRACT:** The formation of binary and ternary model complexes of Eu(III) with the nucleobases 5-aminouracil (5-amino 2,4-dioxy pyrimidine), dihydrouracil (5,6-dihydro-2,4-dioxy pyrimidine), thymine (2,4-dihydroxy 5-methyl pyrimidine), adenine (6-aminopurine), uracil (2,4-dioxy pyrimidine), and PIPES (piperazine 1,4-bis(2-ethane sulfonic acid) disodium salt) has been studied potentiometrically at (25.0 ± 0.1) °C and at an ionic strength of  $I = 0.1 \text{ mol} \cdot \text{dm}^{-3}$  (KNO<sub>3</sub>). The formation of the 1:1, 2:1 binary, and 1:1:1 and 2:1:1 ternary complexes is inferred from the corresponding titration curves. Initial estimates of the formation constants of the resulting species and the protonation constants of the different ligands used have been refined with the SUPERQUAD computer program. The experimental conditions were selected such that self-association of the nucleobases and their complexes was negligibly small; that is, the monomeric and protonated complexes were studied. Recognition of nucleobases and CT-DNA by the luminescent bioprobe Eu(III)–PIPES has been carried out. The solid Eu(III)–PIPES complex was synthesized and characterized using elemental analysis, mass spectra, and IR spectroscopy. The interaction of an aqueous solution of the Eu(III)–PIPES complex with CT-DNA was examined using cyclic voltammetry (CV), differential pulse polarography (DPP), and square wave voltammetry (SWV). The fluorescence emission characteristic band for the Eu(III)–PIPES complex is enhanced by the addition of various concentrations of CT-DNA.

## INTRODUCTION

The sensitive detection of single-stranded regions of DNA, including mutations and mismatches, is critical in nucleic acid hybridization assays with applications that range from the determination of genetic and infectious diseases to providing accurate personal identification.<sup>1–5</sup> Luminescence enhancement of a given probe in the presence of nucleic acids can in principle yield such detection, with marked safety and environmental advantages over radioactive labeling. Owing to the emissive properties of Eu(III) and Tb(III), including their luminescence enhancement through energy transfer<sup>6–10</sup> and their ability to bind single-stranded regions of DNA,<sup>11,12</sup> these ions are potentially valuable for the selective detection of base mismatches.

The luminescence of aqueous Eu(III) and Tb(III) is weak owing to low absorption cross sections and nonradiative deactivation through the O–H vibrations of coordinated water molecules. Therefore, addition of chelating agents or encapsulation of the lanthanide leads to longer emission lifetimes and quantum yields.<sup>13–18</sup> Significantly greater emission intensities can be obtained upon chelation of the ion by ligands that, when excited with light, can transfer energy to the emissive state of the lanthanide. These systems have been probed extensively for potential applications as optical sensors.<sup>19–22</sup> In addition, the emission from lanthanides has proven useful as a sensitive detection method in biological systems and has facilitated their understanding.<sup>23–26</sup> The changes in the intensity of Eu(III) luminescence upon binding to proteins have been utilized to examine the ligation sphere within the active site,<sup>27</sup> whereas distance and conformational information under physiological conditions have been

obtained from energy transfer studies either between two lanthanide ions or from the protein's residues to Eu(III) or Tb(III) bound to the active sites.<sup>28–30</sup>

Single-stranded oligonucleotides are known to enhance the emission of Eu(III) and Tb(III) ions in solution. This feature has been utilized in the detection of distorted DNA regions<sup>31</sup> and to probe DNA– and RNA– drug interactions.<sup>32,33</sup> Lanthanide chelating agents tethered to oligonucleotides have proven important in luminescence energy transfer experiments,<sup>34</sup> as well as in the detection of DNA following complexation of the emissive Eu(III) or Tb(III) ions.<sup>35–37</sup> In addition, the enhancement of lanthanide emission in the presence of DNA with added ligands has been a subject of intense investigation owing to potential application in nucleic acid hybridization assays.<sup>38–40</sup>

In continuation of our previous work on ternary complexes of lanthanides containing biologically important ligands,<sup>41–46</sup> the mixed ligand complexes of the type Eu(III) + nucleobase + PIPES have been investigated by potentiometric pH titrations to determine the formation constants of the normal and protonated mixed ligand complexes formed in solution.

## EXPERIMENTAL SECTION

**Material and Solutions.** All materials employed in the present investigation were of A. R. grade products. [6-Amino purine]

**Received:** September 25, 2010

**Accepted:** February 25, 2011

**Published:** March 14, 2011

C<sub>5</sub>H<sub>5</sub>N<sub>5</sub> (adenine), [5-amino 2,4-dioxy pyrimidine] C<sub>4</sub>H<sub>5</sub>N<sub>3</sub>O<sub>2</sub> (5-aminouracil), [5,6-dihydro-2,4-dioxy pyrimidine] C<sub>4</sub>H<sub>6</sub>N<sub>2</sub>O<sub>2</sub> (dihydrouracil), [5-methyl pyrimidine] C<sub>5</sub>H<sub>6</sub>N<sub>2</sub>O<sub>2</sub> (thymine), [2,4-dioxy pyrimidine] C<sub>4</sub>H<sub>4</sub>N<sub>2</sub>O<sub>2</sub> (uracil), [2-amino-6-oxypurine] C<sub>5</sub>H<sub>5</sub>N<sub>5</sub>O (guanine), and [piperazine 1,4-bis(2-ethane sulfonic acid) dissodium salt] C<sub>8</sub>H<sub>16</sub>N<sub>2</sub>O<sub>6</sub>S<sub>2</sub>Na (PIPES) were purchased from the Sigma Chemical Co. To avoid hydrolysis prior to the potentiometric measurements, a known mass of a chromatographically pure sample of nucleobase as solid was added to a reaction vessel just prior to performing the titration. Eu(NO<sub>3</sub>)<sub>3</sub>·5H<sub>2</sub>O was from the Sigma Chemical Co. The concentrations of the metal ion stock solutions were determined complexometrically by use of ethylenediamine tetracetic acid dissodium salt (EDTA) using suitable indicators.<sup>47</sup>

A CO<sub>2</sub>-free solution of potassium hydroxide (Merck AG) was prepared and standardized against multiple samples of the primary standard potassium hydrogen phthalate (Merck AG) under CO<sub>2</sub>-free conditions. HNO<sub>3</sub> solutions were prepared and standardized potentiometrically with tris(hydroxyl methyl) amino methane. The ionic strength of the studied solutions was adjusted to 0.1 mol·dm<sup>-3</sup> using a stock solution of KNO<sub>3</sub> in potentiometric and spectral measurements. The KNO<sub>3</sub> was from Merck AG. In the electroanalytical measurements, the ionic strength of the examined solutions was adjusted to 0.1 mol·dm<sup>-3</sup> using an alcoholic solution of *p*-toluenesulfonate. This supporting electrolyte was purchased from Merck AG.

**Apparatus and Procedure.** The value of the EMF of the cell was taken with a commercial Fisher Accumet pH/ion meter model 825 MP. The potentiometric system was connected to a glass electrode (Metrohm 1028) connected against a double junction reference electrode (Orion 9020). The temperature was controlled by circulation of water through the jacket from a VEB model E3E ultrathermostat bath and maintained at (25.0 ± 0.1) °C. Purified nitrogen was bubbled through the solution to maintain an inert atmosphere. Efficient stirring of the solution was achieved with a magnetic stirrer. All solutions were prepared in a constant ionic medium, 0.1 mol·dm<sup>-3</sup> KNO<sub>3</sub>.

Gran's method<sup>48</sup> was used to determine  $E^{o'}$  and  $E_j$  so that the hydrogen ion concentration,  $h$ , could be found from  $E$ , the measured potential by means of

$$E \text{ (mV)} = E^{o'} - 59.157 \log h + E_j \quad (1)$$

The protonation constants were then determined by the use of the Bjerrum function.<sup>49</sup>

$$\begin{aligned} \bar{n} &= (H_T - h + K_W/h)/A_T \\ &= (\beta_1 h + 2\beta_2 h^2)/(1 + \beta_1 h + \beta_2 h^2) \end{aligned} \quad (2)$$

which is calculated from the experimental quantities,  $h$ , the total concentration of titratable hydrogen ion,  $H_T$ , and the total reagent concentration,  $A_T$ .  $pK_a$  values of the investigated ligands were determined from the overall protonation constants  $\beta_1$  and  $\beta_2$  calculated by the linearization method of Irving and Rossotti.<sup>50</sup>

Initial estimates of the  $pK_a$  values were refined with the ESAB2M computer program.<sup>51</sup>

A detailed description of the solution compositions used in the determination of the stability constants of complex species is shown in Table 1.

For both ligand protonation and metal complex formation equilibria, data were collected over the largest possible pH interval, although a number of experimental points were

**Table 1. Description of Solution Composition (a–h) Used in the Determination of the Stability Constants of Complex Species Formed**

a	4 · 10 <sup>-4</sup> mol·dm <sup>-3</sup> HNO <sub>3</sub> + 1 · 10 <sup>-4</sup> mol·dm <sup>-3</sup> PIPES (as the first ligand)
b	4 · 10 <sup>-4</sup> mol·dm <sup>-3</sup> HNO <sub>3</sub> + 1 · 10 <sup>-4</sup> mol·dm <sup>-3</sup> nucleobases (adenine, dihydrouracil, 5-aminouracil, thymine, and uracil)
c	solution (a) + 1 · 10 <sup>-4</sup> mol·dm <sup>-3</sup> Eu(III)
d	solution (b) + 1 · 10 <sup>-4</sup> mol·dm <sup>-3</sup> Eu(III)
e	solution (a) + 2 · 10 <sup>-4</sup> mol·dm <sup>-3</sup> Eu(III)
f	solution (b) + 2 · 10 <sup>-4</sup> mol·dm <sup>-3</sup> Eu(III)
g	4 · 10 <sup>-4</sup> mol·dm <sup>-3</sup> HNO <sub>3</sub> + 1 · 10 <sup>-4</sup> mol·dm <sup>-3</sup> PIPES + 1 · 10 <sup>-4</sup> mol·dm <sup>-3</sup> nucleobases + 1 · 10 <sup>-4</sup> mol·dm <sup>-3</sup> Eu(III)
h	4 · 10 <sup>-4</sup> mol·dm <sup>-3</sup> HNO <sub>3</sub> + 1 · 10 <sup>-4</sup> mol·dm <sup>-3</sup> PIPES + 1 · 10 <sup>-4</sup> mol·dm <sup>-3</sup> nucleobases + 2 · 10 <sup>-4</sup> mol·dm <sup>-3</sup> Eu(III)

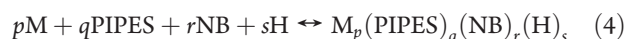
frequently discarded for the final stability constant calculations, especially within the range where the complexation observed was insignificant.

Initial estimates of the formation constants of the ternary complexes and the stability constants of binary 1:1 complexes have been refined using the SUPERQUAD computer program.<sup>51</sup> During this refinement, the stepwise stability constant is

$$K_{M(\text{PIPES})(\text{NB})} = \frac{[M_p(\text{PIPES})_q(\text{NB})_r]}{[M_p(\text{PIPES})_q](\text{NB})^r} \quad (3)$$

which refers to the addition of the nucleobase to the binary complex  $M_p(\text{PIPES})_q$ .

The overall complexation reaction which can also involve protonation is



$$\beta_{pqrs} = \frac{M_p(\text{PIPES})_q(\text{NB})_r(\text{H})_s}{[M]^p[\text{PIPES}]^q[\text{NB}]^r[H]^s} \quad (5)$$

in which NB = nucleobase ligand (5-aminouracil, dihydrouracil, thymine, adenine, and uracil) and M = Eu(III). All side reactions due to metal ion hydrolysis have been included in the calculations.<sup>52,53</sup>

**Electrochemical Measurements.** Cyclic voltammetry (CV), square wave voltammetry (SWV), and differential pulse voltammetry (DPP) are collected using an EG and G Princeton applied research, potentiostat/galvanostat model 263 with a single compartment voltammetric cell equipped with a glassy carbon (GC) working electrode (area = 0.1963 cm<sup>2</sup>) embedded in a resin, a Pt-wire counter electrode, and a Ag/AgCl electrode as the reference electrode. In typical experiments, the sample volume was 25 cm<sup>3</sup>.

The ionic strength of the studied solutions was adjusted to 0.1 mol·dm<sup>-3</sup> using a *para*-toluenesulfonate solution or phosphate buffer.

**Cyclic Voltammetry.** The solution was purged with nitrogen for 120 s, and then the potential was scanned at a scan rate of 100 mV·s<sup>-1</sup> from (-0.30 to -0.90) V and from (1.0 to 0.1) V.

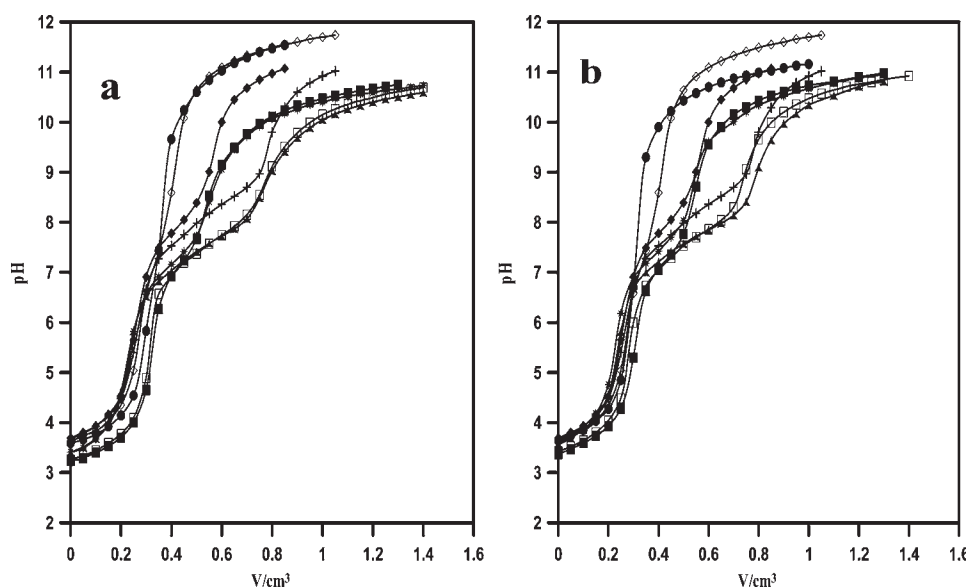


**Figure 1.** pH against volume of  $0.033 \text{ mol}\cdot\text{dm}^{-3}$  KOH for the Eu(III)–PIPES–NB system at  $0.1 \text{ mol}\cdot\text{dm}^{-3}$   $\text{KNO}_3$  and at  $25^\circ\text{C}$ :  $\bullet$ ,  $4\cdot 10^{-4} \text{ mol}\cdot\text{dm}^{-3}$   $\text{HNO}_3$  +  $1\cdot 10^{-4} \text{ mol}\cdot\text{dm}^{-3}$  PIPES;  $\diamond$ ,  $4\cdot 10^{-4} \text{ mol}\cdot\text{dm}^{-3}$   $\text{HNO}_3$  +  $1\cdot 10^{-4} \text{ mol}\cdot\text{dm}^{-3}$  NB;  $\blacksquare$ ,  $4\cdot 10^{-4} \text{ mol}\cdot\text{dm}^{-3}$   $\text{HNO}_3$  +  $1\cdot 10^{-4} \text{ mol}\cdot\text{dm}^{-3}$  PIPES +  $1\cdot 10^{-4} \text{ mol}\cdot\text{dm}^{-3}$  Eu(III);  $\blacklozenge$ ,  $4\cdot 10^{-4} \text{ mol}\cdot\text{dm}^{-3}$   $\text{HNO}_3$  +  $1\cdot 10^{-4} \text{ mol}\cdot\text{dm}^{-3}$  NB +  $1\cdot 10^{-4} \text{ mol}\cdot\text{dm}^{-3}$  Eu(III);  $\square$ ,  $4\cdot 10^{-4} \text{ mol}\cdot\text{dm}^{-3}$   $\text{HNO}_3$  +  $1\cdot 10^{-4} \text{ mol}\cdot\text{dm}^{-3}$  PIPES +  $2\cdot 10^{-4} \text{ mol}\cdot\text{dm}^{-3}$  Eu(III);  $+$ ,  $4\cdot 10^{-4} \text{ mol}\cdot\text{dm}^{-3}$   $\text{HNO}_3$  +  $1\cdot 10^{-4} \text{ mol}\cdot\text{dm}^{-3}$  NB +  $2\cdot 10^{-4} \text{ mol}\cdot\text{dm}^{-3}$  Eu(III);  $*$ ,  $4\cdot 10^{-4} \text{ mol}\cdot\text{dm}^{-3}$   $\text{HNO}_3$  +  $1\cdot 10^{-4} \text{ mol}\cdot\text{dm}^{-3}$  PIPES +  $1\cdot 10^{-4} \text{ mol}\cdot\text{dm}^{-3}$  NB +  $1\cdot 10^{-4} \text{ mol}\cdot\text{dm}^{-3}$  Eu(III);  $\blacktriangle$ ,  $4\cdot 10^{-4} \text{ mol}\cdot\text{dm}^{-3}$   $\text{HNO}_3$  +  $1\cdot 10^{-4} \text{ mol}\cdot\text{dm}^{-3}$  PIPES +  $1\cdot 10^{-4} \text{ mol}\cdot\text{dm}^{-3}$  NB +  $2\cdot 10^{-4} \text{ mol}\cdot\text{dm}^{-3}$  Eu(III). (a) NB = uracil, (b) NB = thymine.

**Square Wave Voltammetry.** The samples were analyzed as in cyclic voltammetry. The pulse height was 25 mV; the SW frequency was  $f = 20$  Hz; and the scan increment was 2.0 mV.

**Differential Pulse Voltammetry.** The samples were analyzed as in cyclic voltammetry but at a scan rate =  $36.6 \text{ mV}\cdot\text{s}^{-1}$ . The pulse height was 25 mV; the pulse width was 50 s; the frequency was 20 Hz; and the scan increment was 2.0 mV.

**Spectrophotometric Measurements.** The UV spectra of the solutions were scanned on a Shimadzu-1601PC UV–visible automatic recording spectrophotometer with 1 cm quartz cells for the absorbance and spectral measurements. All the studied solutions were diluted with bidistilled water, after pH adjustment to the physiological pH using a phosphate buffer (pH = 7.0).

**Spectrofluorometric Measurements.** The emission spectra of the solutions were scanned on a JASCO-FP6300 spectrofluorometer with 1 cm quartz cells. All the studied solutions were diluted with bidistilled water, and the pH was adjusted to the physiological pH using a phosphate buffer solution (pH = 7.0).

**Preparation of Solid Complexes.** The lanthanide complexes were prepared by adding an aqueous solution (ca. 10 mL) of PIPES disodium salt (1.038 g, 3 mmol) to an aqueous solution (ca. 5 mL) of the lanthanide salt ( $\text{Eu}(\text{NO}_3)_3\cdot 5\text{H}_2\text{O}$ , 0.366 g, 1 mmol). After stirring the mixture for 1 h, an aqueous solution (5 mL) containing tetrabutyl ammonium chloride hydrate ( $\text{NBu}_4\text{NCl}\cdot n\text{H}_2\text{O}$ , 1.113 g, 4 mmol) was added, and then the pH of the solution was adjusted using dilute solutions of KOH and  $\text{HNO}_3$  to pH = 3.00. After stirring the mixture for 24 h, a white precipitate formed and was filtered, washed with acetone, and then dried at  $100^\circ\text{C}$ . The synthesized solid complex was characterized by elemental analysis, IR, mass spectrometry, and thermal analysis.

The CHNS elemental analysis was done using a Thermo Flasha Eager 300.

**Table 2.** Formation Constants for the Eu(III) + Nucleobase and Eu(III) + PIPES Binary Complexes and Those for the Mixed Complexes Eu(III) + Nucleobase + PIPES at  $(25.0 \pm 0.1)^\circ\text{C}$  and Ionic Strength  $I = 0.1 \text{ mol}\cdot\text{dm}^{-3}$   $\text{KNO}_3$ <sup>a</sup>

ligand	$\log K_{\text{Eu(III)(NB)}} \text{ and } \log K_{\text{Eu(III)(PIPES)}}$	$\log K_{\text{Eu(III)(NB)(PIPES)}}$
dihydrouracil	$4.28 \pm 0.02$	$7.05^c \pm 0.03$
thymine	$4.28 \pm 0.02$	$10.49^c \pm 0.02$
uracil	$4.29 \pm 0.02$	$7.91^c \pm 0.02$
adenine	$4.27 \pm 0.01$	$4.26^b \pm 0.03$
5-aminouracil	$4.26 \pm 0.01$	$7.58^c \pm 0.01$
PIPES	$4.22 \pm 0.03$	

<sup>a</sup>  $\pm$  refers to three times standard deviation ( $3\sigma$ ). <sup>b</sup> Log formation constants of normal ternary complex. <sup>c</sup> Log formation constants of protonated ternary complex.

The infrared spectra were analyzed using a Perkin-Elmer 1650 FT-IR instrument.

The thermal behavior including differential thermal analysis (DTA), thermogravimetry (TG), and differential thermogravimetry (DTG) was obtained using a Shimadzu DTG-60H in a dynamic air atmosphere ( $40 \text{ mL}\cdot\text{min}^{-1}$ ) at a heating rate of  $10^\circ\text{C}\cdot\text{min}^{-1}$ .

The conductivity of the dissolved complex in distilled water was measured using a Jenco model 1671 Dual Display Bench Top instrument pH/ORP (redox)/conductivity.

## RESULTS AND DISCUSSION

The acid formation constant values for thymine, adenine, uracil, dihydrouracil, 5-aminouracil, and PIPES and the stability constants of their Eu(III)–complexes were determined from the titration curves and are in good agreement with the literature.<sup>54</sup>

In Figure 1a representative set of the experimental titration curves obtained according to the sequence described in the Experimental Section are displayed for the system Eu(III)–PIPES–NB (thymine, adenine, uracil, dihydrouracil, and 5-aminouracil). Generally, the complex titration curves show an inflection after the addition of 2 mol of base per mol of nucleobase. This indicates the stoichiometry of the final product formed in this buffer region.

At the experimental pH values used in calculations in this work, the interfering effects of hydroxyl complexes are negligible for Eu(III). Thus, the protonated secondary ligand combines with the binary 1:1 Eu(III)–nucleobase complexes [Eu(III)–dihyrouracil, Eu(III)–5-aminouracil, Eu(III)–thymine, Eu-

(III)–uracil, Eu(III)–adenine]. The initial estimates of the stability constants of the protonated ternary complexes formed in solution have been determined using half point neutralization. Initial estimates of the stability constants of different normal and protonated monomeric and dimeric binary and ternary complexes formed in solution have been refined with the SUPERQUAD computer program.<sup>51</sup> The quality of the fit during this refinement was judged by the values of the sample standard deviations and the goodness of fit  $\chi^2$  (Pearson's test). At  $\sigma_E = 0.1$  mV (0.001 pH error) and  $\sigma_V = 0.005$  mL, the values of  $S$  in different sets of titrations were between 1.0 and 1.7, and  $\chi^2$  was between 12.0 and 13.0. The scatter of residuals ( $E_{\text{obs}} - E_{\text{calc}}$ ) versus pH was reasonably random, without any significant systematic trends, thus indicating a good fit of the experimental data of the expected model systems under our experimental conditions.

The formation constant values for the binary Eu(III)–nucleobase and ternary Eu(III)–nucleobase–PIPES complexes are collected in Table 2. As shown in the different titration curves, formation of the complexes begins near the pH region from 6 to 6.5. With respect to the nucleobases used, the trend of increasing stability of the binary complexes is as follows: uracil > thymine  $\approx$  dihydrouracil > adenine > 5-aminouracil for the monomeric 1:1 complex species.

For the dimeric Eu(III)–nucleobase (2:1) the stability follows the order: dihydrouracil > thymine  $\approx$  uracil > adenine > 5-aminouracil.

To the author's knowledge, no data for the ternary complex of the secondary ligand PIPES with the nucleobases dihydrouracil,

**Table 3. Formation Constants for the Dimeric Binary Eu(III) + Nucleobase and Eu(III) + PIPES Complexes and Those for the Dimeric Ternary Complexes of Eu(III) + Nucleobase + PIPES at  $(25.0 \pm 0.1)$  °C and Ionic Strength  $I = 0.1 \text{ mol} \cdot \text{dm}^{-3} \text{ KNO}_3$**

ligand	$\log K_{\text{Eu(III)}_2(\text{NB})}$	
	and $\log K_{\text{Eu(III)}_2(\text{PIPES})}$	$\log K_{\text{Eu(III)}_2(\text{NB})(\text{PIPES})}$
dihyrouracil	$4.27 \pm 0.02$	$7.78 \pm 0.01$
thymine	$4.32 \pm 0.02$	$6.09 \pm 0.02$
uracil	$4.32 \pm 0.01$	$5.83 \pm 0.01$
adenine	$4.29 \pm 0.01$	$4.28 \pm 0.02$
5-aminouracil	$4.97 \pm 0.01$	$4.85 \pm 0.01$
PIPES	$4.26 \pm 0.02$	

**Table 4. Analysis Data for the Eu(III)–PIPES Solid Complex**

formula	C %		H %		N %		S %		Eu %		$\Lambda$ (25 °C)
	calc.	found	calc.	found	calc.	found	calc.	found	calc.	found	
$\text{C}_{48}\text{H}_{110}\text{N}_7\text{O}_{18}\text{S}_4\text{Eu}$	42.22	40.23	8.06	7.65	7.18	6.53	9.38	9.07	9.38	9.31	53

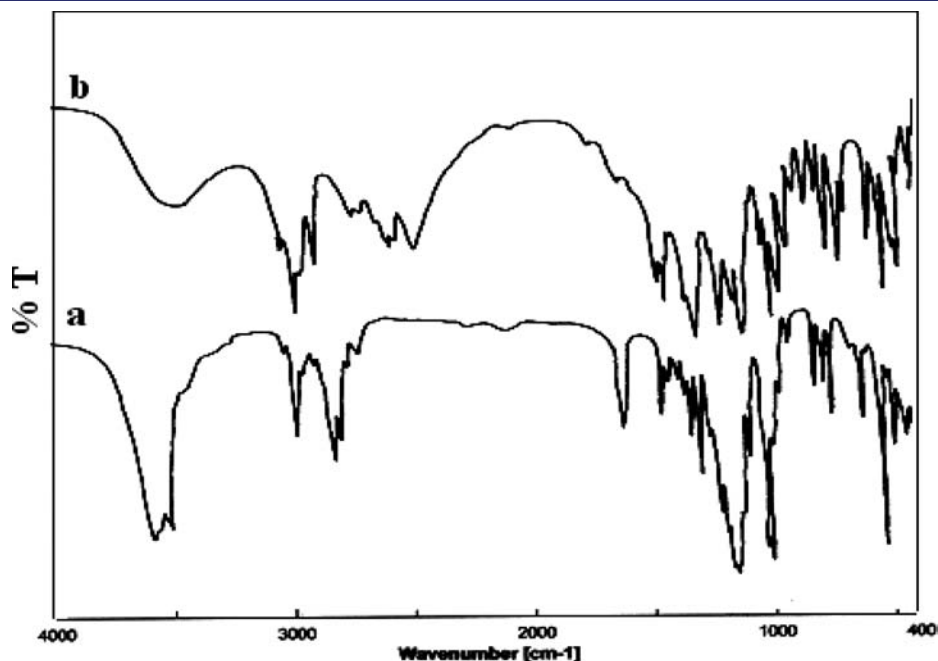


**Figure 2.** IR spectra of (a) PIPES and (b) Eu(III)–PIPES.

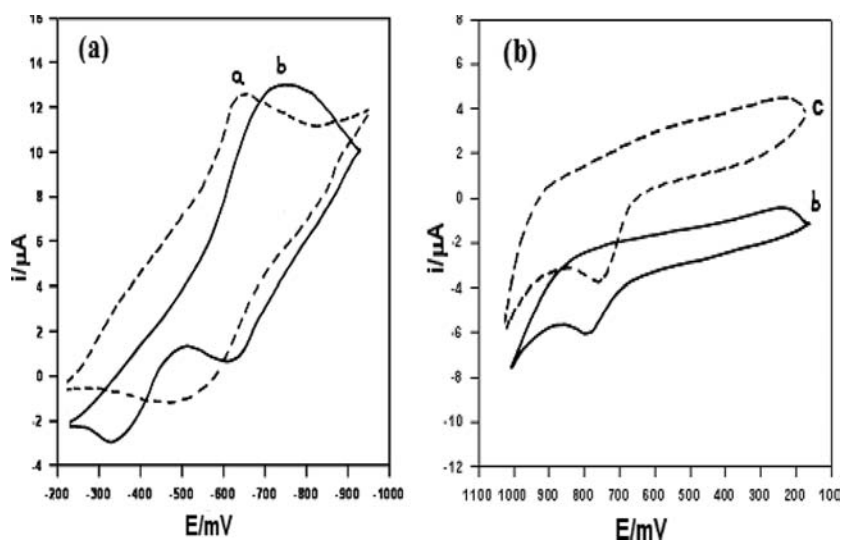


**Figure 3.** Cyclic voltammograms for the Eu(III)–PIPES solid complex and DNA at scan rate =  $100 \text{ mV} \cdot \text{s}^{-1}$  and at  $25.0 \text{ }^\circ\text{C}$  (a) in  $0.1 \text{ mol} \cdot \text{dm}^{-3}$  *p*-toluenesulfonate and (b) in phosphate buffer. (a)  $5 \cdot 10^{-4} \text{ mol} \cdot \text{dm}^{-3}$  Eu(III)–PIPES complex, (b)  $5 \cdot 10^{-4} \text{ mol} \cdot \text{dm}^{-3}$  Eu(III)–PIPES complex +  $5 \cdot 10^{-5} \text{ mol} \cdot \text{dm}^{-3}$  DNA, and (c)  $5 \cdot 10^{-5} \text{ mol} \cdot \text{dm}^{-3}$  DNA.

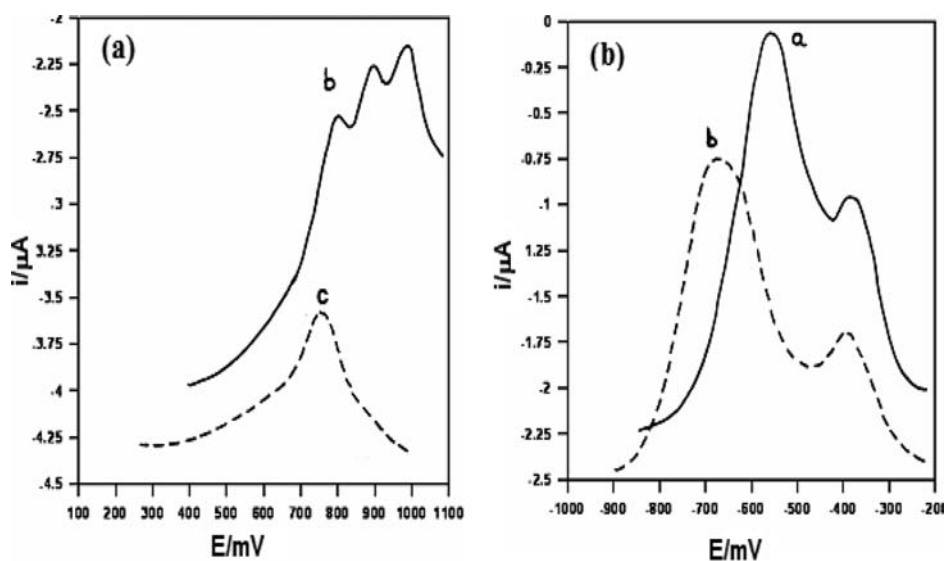


**Figure 4.** Differential pulse polarograms for the Eu(III)–PIPES solid complex and DNA at a scan rate =  $25 \text{ mV} \cdot \text{s}^{-1}$  and at  $25.0 \text{ }^\circ\text{C}$  (a) in phosphate buffer and (b) in  $0.1 \text{ mol} \cdot \text{dm}^{-3}$  *p*-toluenesulfonate. (a)  $5 \cdot 10^{-4} \text{ mol} \cdot \text{dm}^{-3}$  Eu(III)–PIPES complex, (b)  $5 \cdot 10^{-4} \text{ mol} \cdot \text{dm}^{-3}$  Eu(III)–PIPES complex +  $5 \cdot 10^{-5} \text{ mol} \cdot \text{dm}^{-3}$  DNA, and (c)  $5 \cdot 10^{-5} \text{ mol} \cdot \text{dm}^{-3}$  DNA.

5-aminouracil, uracil, thymine, and adenine are available in the literature for comparison.

The formation constants for the Eu(III)–PIPES–nucleobase in a 1:1:1 ratio are calculated based on that the titration curve lies between the corresponding binary curves for Eu(III)–PIPES and Eu(III)–nucleobase (where NB = uracil, thymine, dihydrouracil, 5-aminouracil); i.e., the formed complex species is of the monoprotonated type Eu(III)(PIPES)(HNB) where the nucleobase reacts as a secondary ligand in its protonated form to form ternary complexes with the stability order depending on the nature of the nucleobase: thymine > uracil > 5-aminouracil > dihydrouracil as indicated in Table 2.

The higher values for the stability constants of ternary complexes compared with those of the binary systems may be

attributed to the interligand interactions or some cooperativity between the coordinated ligands, possibly H-bond formation. This also may be explained on the basis of the  $\pi$ -electron donating tendency of the Eu(III) ion to the antibonding  $\pi^*$  orbital of the heteroaromatic N base, such as adenine base, causing strengthening of the Eu(III)–N bond. Due to the back-donation from metal to adenine base, the *f* electrons content on the metal decreases, which renders the metal more electrophilic. The interaction of the  $\pi$  electrons of the secondary ligands with the metal will increase to a greater extent and consequently enhance the formation of the mixed ligand complexes.

Table 3 illustrates the formation constants for the ternary complexes of 2:1:1, where the reaction of Eu(III) with PIPES and

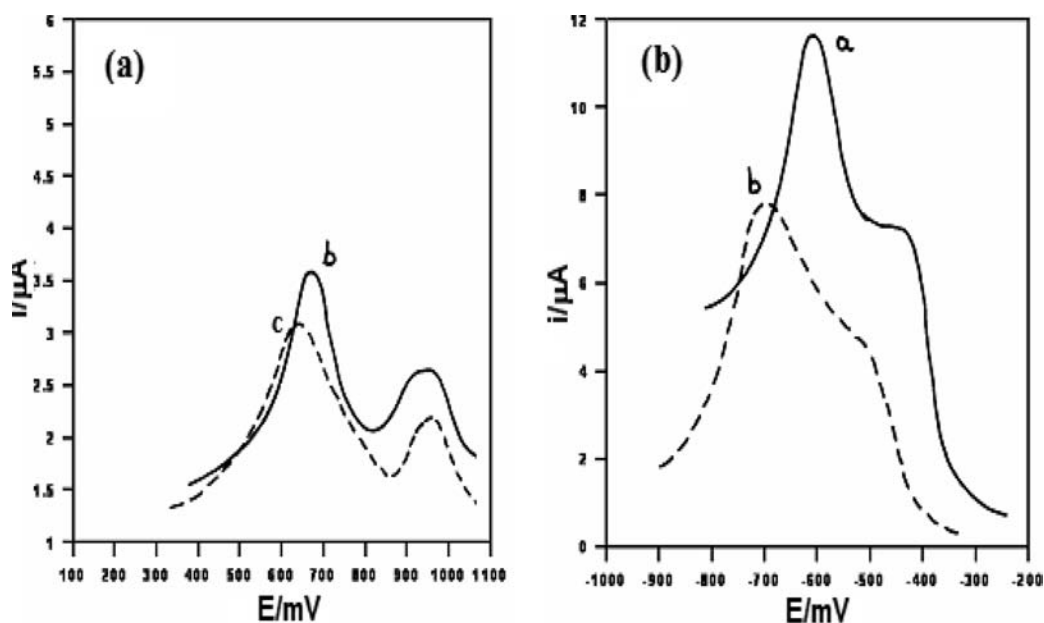


**Figure 5.** Square wave voltammograms for the Eu(III)–PIPES solid complex and DNA at frequency = 20 Hz and at 25.0 °C (a) in phosphate buffer and (b) in 0.1 mol·dm<sup>-3</sup> at *p*-toluenesulfonate. (a) 5·10<sup>-4</sup> mol·dm<sup>-3</sup> Eu(III)–PIPES complex, (b) 5·10<sup>-4</sup> mol·dm<sup>-3</sup> Eu(III)–PIPES complex + 5·10<sup>-5</sup> mol·dm<sup>-3</sup> DNA, and (c) 5·10<sup>-5</sup> mol·dm<sup>-3</sup> DNA.

nucleobases in the dinuclear form will enhance the deprotonation of the nucleobase molecule to form normal complexes of stability order: dihydrouracil > thymine > uracil > 5-aminouracil > adenine.

Taking into consideration the factors which affect metal–nucleobase interactions, which include binding conditions such as pH, temperature, and metal ion concentrations as well as factors associated with the metal ion chemistry, one can account for the trend observed for the stability constants of the different monomeric and dimeric binary and ternary complexes under investigation. Via the formation of mixed-ligand complexes, certain ligand–ligand associations and interactions may be favored, and thus distinct structures may be created in a way that involves only small changes from an energetic point of view.

**Synthesis, Characterization of Eu(III)–PIPES Complex, and Its Interaction with DNA and Its Constituents.** The PIPES molecule has a second stage dissociation constant of 6.80 as detected from the potentiometric measurement at  $I = 0.1$  mol·dm<sup>-3</sup> KNO<sub>3</sub> and at 25 °C.

The synthesized solid complex of Eu(III) with PIPES in a 1:2 ratio exhibits the formula [C<sub>48</sub>H<sub>110</sub>N<sub>7</sub>O<sub>18</sub>S<sub>4</sub>Eu] as confirmed through elemental analysis, mass spectra, IR, and thermal analysis. The analytical data of the complex are depicted in Table 4.

**IR Analysis.** The IR spectrum of the solid Eu(III)–PIPES complex is shown in Figure 2 in comparison with the free ligand, where the latter exhibits bands at (1191 and 1126) cm<sup>-1</sup> which are assigned to the asymmetric sulfonate group (SO<sub>3</sub><sup>-</sup>). The two split bands located at (1056 and 1037) cm<sup>-1</sup> are due to a symmetric type of the SO<sub>3</sub><sup>-</sup> group with probable formation of hydrogen bonding.<sup>55</sup> It is clearly observed that upon coordination of the ligand molecule to Eu(III) the asymmetric and symmetric bands of the SO<sub>3</sub><sup>-</sup> group are shifted to a lower wavenumber. This behavior indicates that the lanthanide metal ion Eu(III) binds to the oxygen atom of the sulfonyl group.

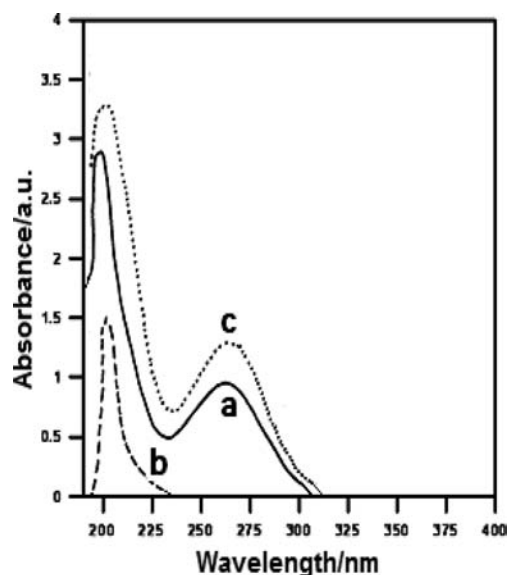


**Figure 6.** Absorption spectra for DNA + [Eu(III)–PIPES] solid complexes in phosphate buffer at 25 °C. (a) —, 5.16·10<sup>-6</sup> mol·dm<sup>-3</sup> DNA; and (c) ····, 5·10<sup>-5</sup> mol·dm<sup>-3</sup> Eu(III)–PIPES complex + 5.16·10<sup>-6</sup> mol·dm<sup>-3</sup> DNA.

The two bands located at (1488 and 1292) cm<sup>-1</sup> could be assigned to the bidentate nature of the nitrate ion.<sup>56</sup>

The complex exhibits a broad band in the region (3330 to 3350) cm<sup>-1</sup> which can be assigned to the coordinated water molecule linked to it.

The molar conductivity of the complex in water indicates that the complex is of a 1:1 electrolyte.

**Thermal Analysis.** The thermal analysis of the synthesized solid complex includes differential thermal analysis (DTA),

thermogravimetry (TG), and differential thermogravimetry (DTG). The DTA curve exhibits a well-defined exothermic peak at 278 °C which may be attributed to the thermal decomposition of the solid complex into the metallic oxide and organic residue. Inspecting the TG curve for the Eu(III)–PIPES solid complex, it is clearly observed that the weight loss that occurs at 148 °C may be attributed to the loss of coordinated water molecules linked to the metal ion, and the weight loss that takes place at 337 °C could be assigned to the decomposition of the organic ligand.

**Interaction of the Eu(III)–PIPES Solid Complex with DNA. Electrochemical Measurements.** The aqueous solution of Eu(III)–PIPES at a concentration of  $5 \cdot 10^{-4} \text{ mol} \cdot \text{dm}^{-3}$  was treated with  $5 \cdot 10^{-5} \text{ mol} \cdot \text{dm}^{-3}$  DNA, and the nature of the

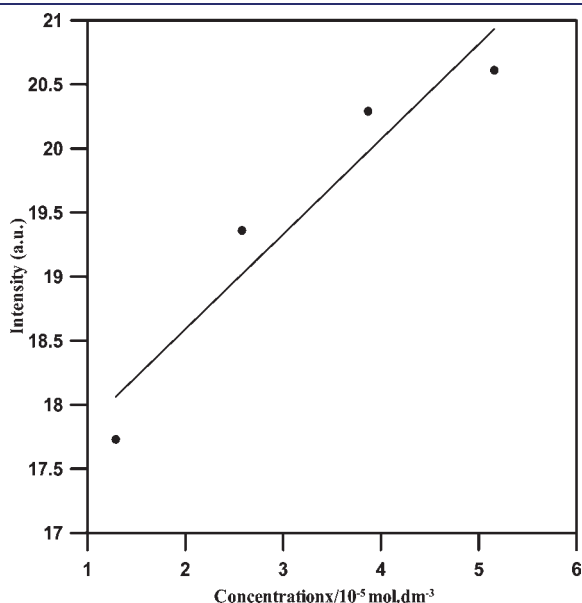


**Figure 7.** Intensity–concentration correlation of CT-DNA with the Eu(III)–PIPES binary complex at at 25 °C.  $[\text{Eu(III)–PIPES}] = 5 \cdot 10^{-4} \text{ mol} \cdot \text{dm}^{-3}$ .  $[\text{ds DNA}] = (1 \cdot 10^{-5} \text{ to } 5 \cdot 10^{-5}) \text{ mol} \cdot \text{dm}^{-3}$ .

interaction was monitored as depicted in Figures 3 to 5 using cyclic voltammetry, differential pulse polarography, and square wave voltammetry.

The dissolved complex was characterized by broad reduction and oxidation waves  $[(-610 \text{ and } -460) \text{ mV}]$ . The reaction of the complex with the DNA molecules reflects itself through the shift of the cathodic potential to more negative (to  $-710 \text{ mV}$ ), i.e., a shift of about 100 mV. In an anodic scan, the broad anodic band is split into two peaks: the first is observed at  $-600 \text{ mV}$ , while the second is located at  $-320 \text{ mV}$  (Figure 3a). The obtained results indicate the strong binding of the complex with the DNA double helix most probably by interaction.

The differential pulse polarogram for Eu(III)–PIPES is characterized by a well-defined reduction peak which is located at a cathodic potential equal to  $-600 \text{ mV}$  and a small peak at  $-560 \text{ mV}$ . The interaction of the dissolved complex in water with the DNA molecule is accompanied by a considerable shift to a more negative direction which agrees well with the cyclic voltammetry results (Figure 4b). A parallel result is obtained from the square wave voltammetric measurements as shown in Figure 5b. The oxidation of the DNA molecule on the surface of the glassy carbon electrode is shown in Figure 3b, where the cyclic voltammograms for DNA are characterized by an anodic peak at 790 mV which could be attributed to the oxidation of the guanine moiety in DNA. The reaction of the dissolved Eu(III)–PIPES with DNA is accompanied by a slight positive shift which indicates the specific binding of the complex to the guanine part in the DNA molecule.

The oxidation of the DNA molecule is characterized by only one peak in the differential pulse polarogram (DPP), and the reaction of DNA with Eu(III)–PIPES causes splitting and perturbation of the oxidation peak specified to the guanine residue into three peaks with positive shifts of the anodic potential (Figure 4a).

Figure 5a illustrates the square wave voltammograms for DNA and the interaction of DNA with the dissolved solid complex Eu(III)–PIPES. The DNA is oxidized on the surface of the glassy carbon electrode through two well-defined peaks: the first

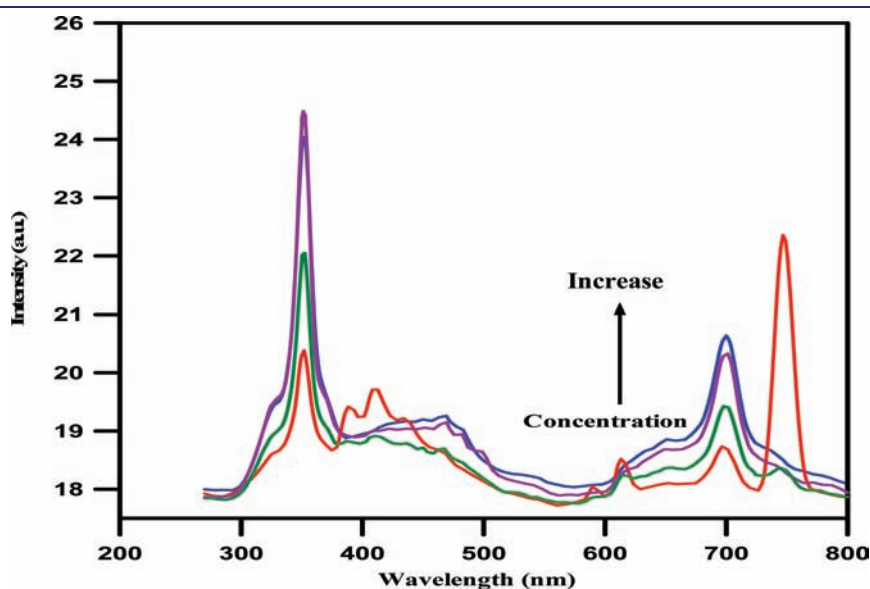


**Figure 8.** Emission spectra for  $5 \cdot 10^{-4} \text{ mol} \cdot \text{dm}^{-3}$  of the Eu(III)–PIPES binary complex with CT-DNA in a concentration range of  $(1 \cdot 10^{-4} \text{ to } 5 \cdot 10^{-4}) \text{ mol} \cdot \text{dm}^{-3}$ .

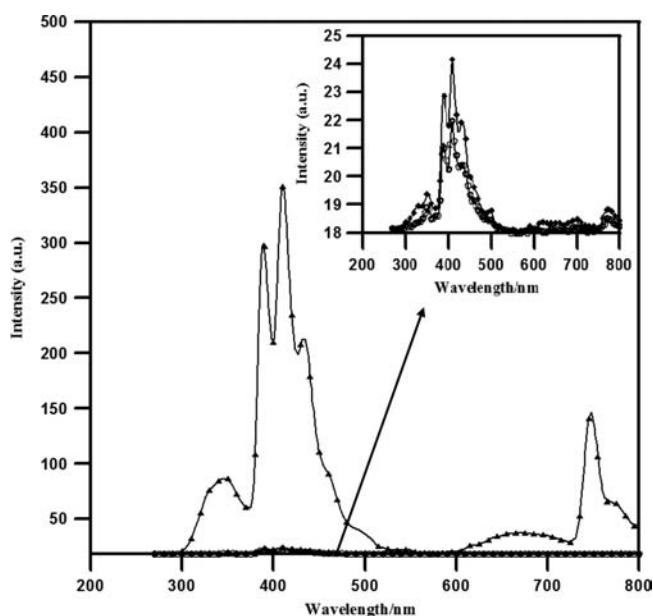


**Figure 9.** Emission spectra for the  $5 \cdot 10^{-4} \text{ mol} \cdot \text{dm}^{-3}$  Eu(III)–PIPES binary complex with the nucleobase (NB) in aqueous medium and at  $25 \text{ }^\circ\text{C}$ .  $\diamond$ ,  $5 \cdot 10^{-4} \text{ mol} \cdot \text{dm}^{-3}$  of Eu(III)–PIPES +  $5 \cdot 10^{-4} \text{ mol} \cdot \text{dm}^{-3}$  adenine;  $\blacklozenge$ ,  $5 \cdot 10^{-4} \text{ mol} \cdot \text{dm}^{-3}$  of Eu(III)–PIPES +  $5 \cdot 10^{-4} \text{ mol} \cdot \text{dm}^{-3}$  thymine;  $\circ$ ,  $5 \cdot 10^{-4} \text{ mol} \cdot \text{dm}^{-3}$  of Eu(III)–PIPES +  $5 \cdot 10^{-4} \text{ mol} \cdot \text{dm}^{-3}$  uracil;  $\blacktriangle$ ,  $5 \cdot 10^{-4} \text{ mol} \cdot \text{dm}^{-3}$  of Eu(III)–PIPES +  $5 \cdot 10^{-4} \text{ mol} \cdot \text{dm}^{-3}$  guanine.

could be attributed to the oxidation of the guanine residue, while the second which is located at +980 mV could be assigned to adenine oxidation. The reaction of the complex with DNA causes a positive shift of the oxidation potential of guanine. On the contrary, the adenine oxidation peak is negative shifted; i.e., the specific binding of Eu(III)–PIPES is with the guanine residue.

**Spectral Measurements.** The double strand calf thymus DNA is characterized by a band at 260 nm, where the Eu(III)–PIPES complex dissolved in water is characterized by an absorption peak in the far UV region. The interaction of the complex with DNA causes an enhancement of the characteristic absorption peak for the DNA as depicted in Figure 6.

Figure 8 illustrates the fluorescence spectra for Eu(III)–PIPES dissolved in water at a concentration of  $5 \cdot 10^{-4} \text{ mol} \cdot \text{dm}^{-3}$ , after excitation at  $\lambda = 250 \text{ nm}$  where an emission band is observed at 690 nm which could be assigned to a  ${}^5\text{D}_0 \rightarrow {}^7\text{F}_4$  transition type, where the intensity of this peak varies with the concentration of DNA within the concentration range ( $1 \cdot 10^{-5}$  to  $5 \cdot 10^{-5}$ )  $\text{mol} \cdot \text{dm}^{-3}$ . The correlation between the concentration of DNA and intensity of the emission peak is shown in Figure 7.

The interaction of the four nucleobases (guanine, adenine, uracil, and thymine) with the Eu(III)–PIPES complex dissolved in water is shown in Figure 9, where it is clearly observed that the reaction of the studied nucleobases with the complex is accompanied by an increase in the emission peak intensity at  $\lambda = 750 \text{ nm}$ . The increase in intensity is low for adenine, uracil, and thymine, but the increase of this peak intensity is considerable in the case of the guanine residue. This result is a good indication of the targeting effect of the Eu(III)–PIPES complex toward the guanine nucleobase either in its form or in the double strand molecule.

## CONCLUSION

During the present study, confirmation of the formation of binary and ternary complexes of Eu(III) with nucleobases 5-aminouracil (5-amino 2,4-dioxy pyrimidine), dihydrouracil (5,6-dihydro-2,4-dioxy pyrimidine), thymine (2,4-dihydroxy 5-methyl pyrimidine), adenine (6-aminopurine), uracil (2,4-dioxy pyrimidine), and PIPES (piperazine 1,4-bis(2-ethane sulfonic acid) disodium salt) in solution has been carried out using cyclic voltammetry (CV), differential pulse polarography (DPP), and square wave voltammetry (SWV). This provides a good support for our potentiometric studies for the formation of monomeric and dimeric binary and ternary complexes in solution. It is quite interesting to observe that changing the frequency from (30 to 60) Hz resulted in a quite clear change in the shape of the SWV of the ternary complex formed in solution, which may be attributed to changing the mechanistic behavior of the electrochemical reduction of the resulting ternary complex at the glassy carbon electrode. On the basis of our electrochemical and fluorescence studies, it was concluded that our synthesized Eu(III)–PIPES has promising affinity to interact with CT-DNA.

## AUTHOR INFORMATION

### Corresponding Author

\*E-mail: azab2@yahoo.com.

## REFERENCES

- (1) (a) Landegren, U., Ed. *Laboratory Protocols for Mutation Detection*; Oxford University Press: New York, 1996. (b) Obe, G.; Nataraja, A. T., Eds. *Chromosomal Alterations: Origin and Significance*; Springer-Verlag: New York, 1994. (c) Davies, K. E.; Read, A. P. *Molecular Basis of Inherited Disease*; Oxford University Press: New York, 1992.
- (2) Jackson, B. A.; Barton, J. K. Recognition of DNA Base Mismatches by a Rhodium Intercalator. *J. Am. Chem. Soc.* **1997**, *119*, 12986–12987.
- (3) Saha, A. K.; Kross, K.; Kloszewski, E. D.; Upson, D. A.; Toner, J. L.; Snow, R. A.; Black, C. D. V.; Desai, V. C. Time Resolved Fluorescence of A New Europium Chelate Complex: Demonstration of Highly Sensitive Detection of Protein and DNA. *J. Am. Chem. Soc.* **1993**, *115*, 11032–11033.
- (4) Lippert, B. Effects of Metal-Ion Binding on Nucleobase Pairing: Stabilization, Prevention and Mismatch Formation. *J. Chem Soc., Dalton Trans* **1997**, 3971–3976.
- (5) Oser, A.; Valet, G. Nonradioactive Assay of DNA Hybridization by DNA-Template-Mediated Formation of a Ternary Tb(III) Complex in Ppure Liquid Phase. *Angew. Chem., Int. Ed. Engl.* **1990**, *29*, 1167–1169.
- (6) Weissman, S. I. Intramolecular Energy Transfer. The Fluorescence of Complexes of Europium. *J. Chem. Phys.* **1942**, *10*, 214–217.
- (7) Crosby, G. A. Luminescent Organic Complexes of The Rare Earths. *Mol. Cryst.* **1966**, *1*, 37–81.
- (8) Sato, S.; Wada, M. Relation Between Intramolecular Energy Transfer Efficiencies and Triplet State Energies in Rare Earth  $\beta$ -Diketone Chelate. *Bull. Chem. Soc. Jpn.* **1970**, *43*, 1955–1962.
- (9) Waston, W. M.; Zerger, R. P.; Yardley, J. T.; Stucky, G. D. Examination of Photophysics in Rare Earth Chelates by Laser-Excited Luminescence. *Inorg. Chem.* **1975**, *14*, 2675–2680.
- (10) Li, M.; Selvin, P. R. Luminescent Polyaminocarboxylate Chelates of Terbium and Europium: The Effect of Chelate Structure. *J. Am. Chem. Soc.* **1995**, *117*, 8132–8138.
- (11) Klakamp, S. L.; Horrocks, W. D., Jr. Lanthanide Ion luminescence as a Probe of DNA Structure. 1. Guanine-Containing Oligomers and Nucleotides. *J. Inorg. Biochem.* **1992**, *46*, 175–205.



- (12) Topal, M. D.; Fresco, J. R. Fluorescence of Terbium Ton-Nucleic Acid Complexes: A Sensitive Specific Probe for Unpaired Residues in Nucleic Acids. *Biochemistry* **1980**, *19*, 5531–5537.
- (13) Sabbatini, N.; Guardigli, M.; Lehn, J.-M. Luminescent Lanthanide Complexes as Photochemical Supramolecular Devices. *Coord. Chem. Rev.* **1993**, *123*, 201–228.
- (14) (a) Rigault, S.; Piguet, C.; Bernardinelli, G.; Hopfgartner, G. Metal-Lanthanide-Assisted of an Inert, Metal-Containing Nonadentate Tripodal Receptor. *Angew. Chem., Int. Ed. Engl.* **1998**, *37*, 169–172. (b) Martin, N.; Bünzli, I.-C. G.; McKee, V.; Piguet, C.; Hopfgartner, G. Self-Assembled Dinuclear Lanthanide Helicates: Substantial Luminescence Enhancement upon Replacing Terminal Benzimidazole Groups by Carboxamide Binding Units. *Inorg. Chem.* **1998**, *37*, 577–589. (c) Piguet, C.; Bünzli, I.-C. G.; Bernardinelli, G.; Hopfgartner, G.; Petoud, S.; Schaad, O. Lanthanide Podates with Predetermined Structural and Photophysical Properties: Strongly Luminescent Self-Assembled Heterodinuclear d-f Complexes with a Segmental Ligand Containing Heterocyclic Imines and Carboxamide Binding Units. *J. Am. Chem. Soc.* **1996**, *118*, 6681–6697.
- (15) Alexander, V. Design and Synthesis of Macrocyclic Ligands and Their Complexes of Lanthanides and Actinides. *Chem. Rev.* **1995**, *95*, 273–342.
- (16) Choppin, G. R.; Wang, Z. M. Correlation Between Ligand Coordination-Number and the Shift of the F-7(0)-5D(0) Transition Frequency in Europium(III) Complexes. *Inorg. Chem.* **1997**, *36*, 249–252.
- (17) Valente, P.; Lincoln, S. F.; Wainwright, K. P. External Coordination of Europium(III) Prior to Its Encapsulation Within Aa Cyclen-Based Pendant Macrocyclic. *Inorg. Chem.* **1998**, *37*, 2846–2847.
- (18) Wolbers, M. P. O.; van Veggel, F. C. J. M.; Snellink-Ruël, B. H. M.; Hofstra, J. W.; Geurts, F. A. J.; Reinhoudt, D. N. A Novel Preorganized Hemispherand to Encapsulate Rare Earth Ions: Shielding and Ligand Deuteriation for Prolonged Lifetimes of Excited  $\text{Eu}^{3+}$  Ions. *J. Am. Chem. Soc.* **1997**, *119*, 138–144.
- (19) (a) deSilva, A. P.; Gunaratne, H. Q. N.; Gunnlaugsson, T.; Huxley, A. J. M.; McCoy, C. P.; Rademacher, J. T.; Rice, T. E. Signaling Recognition Events with Fluorescent Sensors and Switches. *Chem. Rev.* **1997**, *97*, 1515–1566. (b) deSilva, A. P.; Gunaratne, H. Q. N.; McCoy, C. P. A Molecular Photoionic and Gate Based on Fluorescent Signalling. *Nature* **1993**, *364*, 42–44.
- (20) (a) Rudzinski, C. M.; Engebretson, D. S.; Harman, W. K.; Nocera, D. G. Mechanism for The Sensitized Luminescence of A Lanthanide Ion Macrocyclic Appended to a Cyclodextrin. *J. Phys. Chem. A* **1998**, *102*, 7442. (b) Mortellaro, M. A.; Nocera, D. G. A Supramolecular Chemosensor for Aromatic Hydrocarbons. *J. Am. Chem. Soc.* **1996**, *118*, 7414–7415.
- (21) (a) Parker, D.; Williams, J. A. G. Taking Advantage of The pH and  $\text{pO}_2$  Sensitivity of A Macrocyclic Terbium Phenanthridinium Complex. *Chem. Commun.* **1998**, 245–246. (b) Gunnlaugsson, T.; Parker, D. Luminescent Europium Tetraazamacrocyclic Complexes with Wide Range pH Sensitivity. *Chem. Commun.* **1998**, 511–512. (c) Parker, D.; Senanayake, K.; Williams, J. A. G. Luminescent Chemosensors for pH, Halide and Hydroxide Ions Based on Kinetically Stable, Macrocyclic Europium -Phenanthridinium Conjugates. *Chem. Commun.* **1997**, 1777–1778.
- (22) Ghosh, P.; Bharadwaj, P. K.; Roy, J.; Ghosh, S. Transition Metal (II)/(III), Eu(III) and Tb(III) Ions Induced Molecular Photoionic or Gates Using Trianthryl Cryptands of Varying Cavity Dimension. *J. Am. Chem. Soc.* **1997**, *119*, 11903–11909.
- (23) Horrocks, W. D., Jr.; Bolender, J. P.; Smith, W. D.; Supkowski, R. M. Photosensitized Near Infrared Luminescence of Terbium (III) in Proteins and Complexes Occurs Via an Internal Redox Process III. *J. Am. Chem. Soc.* **1997**, *119*, 5972–5973.
- (24) Diamandis, E. P.; Christopoulos, T. K. Fluoroimmunoassays and Immunofluorometric Assays. *Anal. Chem.* **1990**, *62*, 1149–1157.
- (25) Elbnowski, M.; Makowska, B. The Lanthanides as Luminescent Probes in Investigations of Biochemical Systems. *J. Photochem. Photobiol. A* **1996**, *99*, 85–92.
- (26) Meskers, S. C. J.; Dekkers, H. P. J. M. Binding of Vitamin B-12 and B-12a to an Antibody and to Haptocorrin Probed by Enantioselective Quenching of Tb(Pyridine-2,6-Dicarboxylate)(3)(3-) Luminescence. *J. Am. Chem. Soc.* **1998**, *120*, 6413–6414.
- (27) (a) Frey, S. T.; Gong, M. L.; Horrocks, W. D. Synergistic Coordination in Ternary Complexes of  $\text{Eu}^{3+}$  with Aromatic Beta-Diketone Ligands and 1,10-Phenanthroline. *Inorg. Chem.* **1994**, *33*, 3229–3234.
- (28) (a) Chaudhuri, D.; Horrocks, W. D., Jr.; Amburgey, J. C.; Weber, D. J. Characterization of Lanthanide Ion Binding to The EF-Hand Protein S100 Beta by Luminescence Spectroscopy. *Biochemistry* **1997**, *36*, 9674–9680. (b) Frey, S. T.; Gong, M. L.; Horrocks, W. D., Jr. Synergistic Coordination in Ternary Complexed of  $\text{Eu}^{3+}$  with Aromatic Beta-Diketone Ligands and 1.10-Phenanthroline. *Inorg. Chem.* **1994**, *33*, 3229–3234.
- (29) Schlyer, B. D.; Steel, D. G.; Gafni, A. Direct kinetic Evidence for Triplet State Energy Transfer From Escherichia Coli Alkaline Phosphatase Tryptophan 109 to Bound Terbium. *J. Biol. Chem.* **1995**, *270*, 22890–22894.
- (30) Cierniewski, C. S.; Hass, T. A.; Smith, J. W.; Plow, E. F. Characterization of Cation-Binding Sequences in The Platelet Integrin GPIIb-IIIa ( $\alpha\text{IIb}\beta_3$ ) by Terbium Luminescence. *Biochemistry* **1994**, *33*, 12238–12246.
- (31) Balcarová, Z.; Brabec, V. Reinterpretation of Fluorescence of Terbium Ion-DNA Complexes. *Biophys. Chem.* **1989**, *33*, 55–61.
- (32) Pearlman, L. F.; Simpkins, H. The Differential Effects Produced by Daunomycin and Adriamycin on RNA, polynucleotides, Single Stranded, Supercoiled DNA, and Nucleosomes. *Biochem. Biophys. Res. Commun.* **1985**, *131*, 1033–1040.
- (33) Ci, Y.-X.; Li, Y.-Z.; Liu, X. Selective Determination of DNA by Its Enhancement Effect on The Fluorescence of The  $\text{Eu}^{3+}$ -Tetracycline complex. *J. Anal. Chem.* **1995**, *67*, 1785–1788.
- (34) Selvin, P. R.; Hearst, J. E. Luminescence Energy Transfer Using a Terbium Chelate: Improvements on Fluorescence Energy Transfer. *Proc. Natl. Acad. Sci. U.S.A.* **1994**, *91*, 10024–10028.
- (35) Li, M.; Selvin, P. R. Amine-Reactive Forms of A Luminescent Diethylenetriaminepentaacetic Acid Chelate of Terbium and Europium: Attachment to DNA and Energy Transfer Measurements. *Bioconjugate Chem.* **1997**, *8*, 127–132.
- (36) Ionannou, P. C.; Christopoulos, T. K. Two-Round Enzymatic Amplification Combined with Time-Resolved Fluorometry of  $\text{Tb}^{3+}$  Chelates for Enhanced Sensitivity in DNA Hybridization Assays. *Anal. Chem.* **1998**, *70*, 698–702.
- (37) Hurskainen, P.; Dahlén, P.; Ylikoski, J.; Kwiatkowski, M.; Siitari, H.; Lövgren, T. Preparation of Europium-Labelled DNA Probes and Their Properties. *Nucleic Acids Res.* **1991**, *19*, 1057–1061.
- (38) Lim, M. J.; Patton, W. F.; Lopez, M. F.; Spofford, K. H.; Shojae, N.; Shepro, D. A Luminescent Europium Complex for the Sensitive Detection of Proteins and Nucleic Acids Immobilized on Membrane Supports. *Anal. Biochem.* **1997**, *245*, 184–195.
- (39) Ci, Y.-X.; Li, Y.-Z.; Chang, W.-B. Fluorescence Enhancement of Terbium(III) by Nucleotides and Polyhomonucleotides in The Presence of Phenanthroline. *Fresenius' J. Anal. Chem.* **1992**, *342*, 91–94.
- (40) Welcher, F. J. *The Analytical Uses of Ethylene Diaminetetraacetic Acid*; D. Von. Nostrand Co., Inc.: Princeton, 1965.
- (41) Azab, H. A.; Orabi, A. S.; ElDeghidy, F. S.; Said, H. Ternary Complexes of La (III), Ce (III), Pr (III) or Er (III) with adenosine 5'-mono, 5'-di, and 5'-triphosphate as primary ligands and some biologically important zwitterionic buffers as secondary ligands. *J. Solution Chem.* **2010**, *3*, 319–334.
- (42) Azab, H. A.; Abd El-Gawad, I. I.; Kamel, R. M. Ternary Complexes Formed by the Fluorescent Probe Eu (III)-9-Anthracene Carboxylic Acid with Pyrimidine and Purine Nucleobases. *J. Chem. Eng. Data* **2009**, *54*, 3069–3078.
- (43) Azab, H. A.; El-Korashy, S. A.; Anwar, Z. M.; Hussein, B. H. M.; Khairy, G. M. Eu (III)-anthracene-9-carboxylic acid as a responsive luminescent bioprobe and its electroanalytical Interactions with N-acetyl

amino acids, nucleotides and DNA. *J. Chem. Eng. Data* **2010**, *55*, 3130–3141.

(44) Azab, H. A.; AboElNour, K. M.; Sherif, S. Metal Ion Complexes Containing Di-, Tripeptides and biologically important zwitterionic buffers. *J. Chem. Eng. Data* **2007**, *52* (2), 381–390.

(45) Anwar, Z. M.; Azab, H. A.; Sokar, M. Metal ion complexes containing nucleobases and some zwitterionic buffers. *J. Chem. Eng. Data* **2004**, *49* (1), 62–72.

(46) Anwar, Z. M.; Azab, H. A. Ternary complexes formed by trivalent lanthanide ions, nucleotides and biological buffers. *J. Chem. Eng. Data* **2001**, *46*, 613–618. Prat, O.; Lopez, E.; Mathis, G. Europium-(III) Cryptate: A Fluorescent Label for the Detection of DNA Hybrids on Solid Support. *Anal. Biochem.* **1991**, *195*, 283–289.

(47) Gran, G. Determination of the Equivalence Point in Potentiometric Titration Part II. *Analyst* **1952**, *77*, 661.

(48) Bjerrum, J. *Metal Amine Complex Formation in Aqueous Solution*; Haase: Copenhagen, 1941.

(49) Irving, H.; Rossotti, H. S. The Calculation of Formation Curves of Metal Complexes from pH-Titration Curves in Mixed Solvents. *J. Chem. Soc.* **1954**, 2904–2910.

(50) De Stefano, C.; Princi, P.; Rigano, C.; Sammartano, S. Computer Analysis of Equilibrium Data in Solution. ESAB2M: An Improved Version of The ESAB Program. *Ann. Chim. (Rome)* **1987**, *77*, 643–675.

(51) Gans, P.; Sabatini, A.; Vacca, A. SUPERQUAD: An Improved General Program for Computation of Formation Constants from Potentiometric Data. *J. Chem. Soc., Dalton Trans.* **1985**, 1195–1200.

(52) Ringbom, A. *Complexation in Analytical Chemistry*; Wiley-Interscience: New York, 1963.

(53) Perrin, D. D.; Dempsey, B. *Buffer for pH and Metal Ion Control*; Chapman and Hall: London, 1979.

(54) Martell, A. E.; Sillen, L. G. *Stability Constants of Metal Ion Complexes*; The Chemical Society: London, 1971.

(55) Sun, B.; Zhao, Y.; Yang, G. C.; Xu, G. X. Crystal Structure and FT-IR Study of Cesium 4-Methylbenzenesulfonate. *J. Mol. Struct.* **1998**, *471*, 1–3.

(56) Nakamoto, K. *Infrared and Raman Spectra of Inorganic and Coordination Compounds*, 3rd ed.; John Wiley: New York, 1973; p 227.